2023 IMEKO TC-4 International Conference on
Metrology for Archaeology and Cultural Heritage
Rome, Italy, October 19-21, 2023

Characterization of Roman Amphora Sherds Using Terahertz Time-of-Flight Tomography

Min Zhai[1,2], Alexandre Locquet[1,2], Haolian Shi[1,2], Cesar Carreras Monfort[3], D.S. Citrin[1,2,*]

[1] *Georgia Tech-CNRS IRL2958, Georgia Tech Europe, 2 Rue Marconi, 57070 Metz France*
[2] *School of Electrical and Computer Engineering, Georgia Institute of Technology, Atlanta, GA 30332, USA*
[3] *Department de Ciències de l'Antiguitat I de l'Edat Mitjana, Universitat Atònoma de Barcelona, Edifici B Facultata de Filosofia I Lletres, 08193 Bellaterra (Barcelona), Spain*
✉: david.citrin@ece.gatech.edu

***Abstract* – Amphorae were pottery containers used for bulk-commodity transport in the Roman Empire. They provide direct evidence for the inter-regional and long-distance movement of agricultural products in the Roman Empire. In general, a whitish skin produced by the deposition of calcite and NaCl in the clay, is often present on the outer surface of Roman amphorae produced in regions with salt-bearing clay or when made with salt water. We employ terahertz reflective imaging with sparse deconvolution for the stratigraphic characterization of Roman amphora sherds excavated from Southern Italy, Southern Spain, and Northern Africa. A skin with a thickness between ~30 and 40 µm was found on the exterior of the sherds.**

I. INTRODUCTION

Amphorae were mostly used for long-distance transport of agricultural products (such as wine, olive oil, fruit, and fish) in the Roman Empire, and the form was derived from earlier Greek examples. Amphorae are one of the most common archaeological items excavated from Roman sites and shipwrecks. Evaluating the source and type of amphora sherd may affect the understanding of an archaeological site and contribute to a deeper understanding of Roman long-distance trade. In addition, as an index of Roman economic activity and seaborne trade, exploring the distribution of amphorae also helps to understand Roman production, consumption, demography, and economy [1-3].

Although Roman amphorae are typically unglazed, a whitish skin is frequently present on the exterior. Reference [4] first showed that this white surface layer is neither paint nor slip but is chemically induced and is associated with the presence of calcite and NaCl in or added to the clay prior to firing. The depletion of magnetite near the surface that occurs during firing leads to the occurrence of whitish skin. At present, there is little known about the thickness of the skin [5], nor is it clear if the skin presents a gradual or abrupt interface.

Chemical and physical characterization of amphorae can help pin down the origin and use. Petrology is the most widely used technique for determining the mineral composition and potential sources, as the source of materials is usually close to the place of production. while epigraphic, chemical, physical, and petrographic studies have led to progress in understanding production, consumption, and trade, less attention has been paid to quantitative aspects of the surface, particularly to the skin. Moreover, as a destructive evaluation approach, the utilization of a polarizing microscope for petrographic requires the destructive extraction of thin sections from Roman amphorae. Therefore, one novel approach that is capable of quantitative characterizing skin in a non-destructive and contactless manner is highly demanded.

Terahertz (THz) electromagnetic waves, whose frequency range by convention is 0.1-10 THz (corresponding to 3000 µm-30 µm in wavelength), lie at the border between the photonic and microwave ranges of the electromagnetic spectrum. THz waves can penetrate many electrically insulating materials that may be otherwise opaque to visible and near-infrared light, thus providing ways to explore the three-dimensional structure of objects. In addition, as non-ionizing radiations, THz waves present minimal known health risks. Due to these combined properties, THz-based techniques have already been successfully applied to investigate numerous art and archaeological objects, such as easel painting, oil painting, papyrus, ceramics, wall painting, mummies, fabric, and manuscripts [6-13].

In this work, we employed THz time-domain spectroscopy to characterize ancient Roman amphora sherds excavated from Northern Africa, Southern Spain, and Southern Italy. A post processing technique, named sparse deconvolution, and based on an iterative shrinkage/thresholding algorithm, is also implemented to determine the skin thickness, and reveal the stratigraphy of the Roman amphora sherds studied.

II. SAMPLE DESCRIPTION

Figure 1 presents photographs of three Roman amphora

sherds studied in this work. The sherd excavated from Northern Africa was probably produced in the region close to Carthage (present coastal Tunis) and is well-dated between 180-120 BCE. The sherd excavated from Southern coastal Spain was probably produced from the Atlantic coast of the present Cadiz and has a wider chronological range between 200 and 100 BCE. The sherd excavated from Campania was probably produced not far from present-day Naples between 180-120 BCE. All sherds studied present a white slip on the exterior surface.

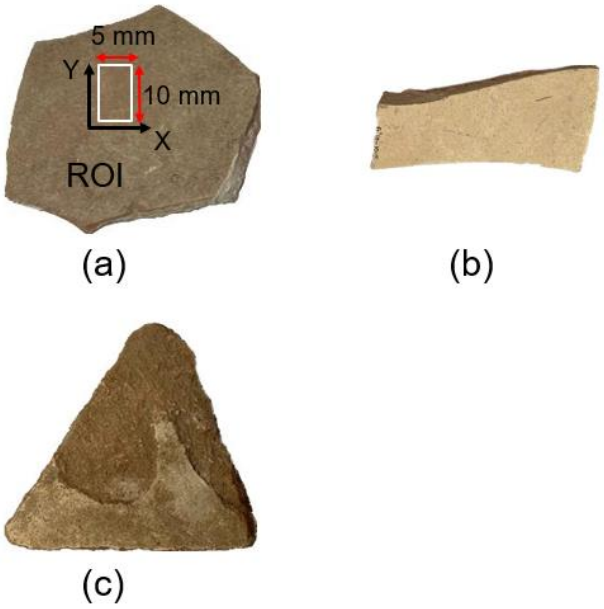

Fig. 1. Photograph of Roman amphora sherds from (a) Northern Africa, (b) Southern Spain, and (c) Southern Italy. White rectangle (10×5 mm^2) in (a) indicates area studied for characterizing stratigraphy and the x and y axis are labeled for Fig. 5.

III. EXPERIMENTAL SETUP

A commercial TPS spectra 3000 from TeraView Ltd., Cambridge, UK is employed for THz reflection measurements. Figure 2 shows the photograph and the schematic diagram of the THz system for reflection mode. The generation of THz pulsed radiation is based on a photoconductive switch. Quasi-single-cycle THz pulses with bandwidth 60 GHz to 3 THz are generated in a biased GaAs antenna excited by an Er-doped fiber laser emitting sub-100-fs 780-nm pulses at 100 MHz repetition rate with average output power > 65 mW. Coherent detection of the reflected THz radiation is performed in a similar photoconductive-antenna circuit. By gating the photoconductive gap with an *fs* pulse synchronized to the THz emission, a current proportional to the THz electric field is measured. A delay line is used to change the difference in the optical delay between the incoming THz pulse and the probe laser pulse at the receiver. A bias is also applied across the emitter and receiver to generate a time-gated output signal.

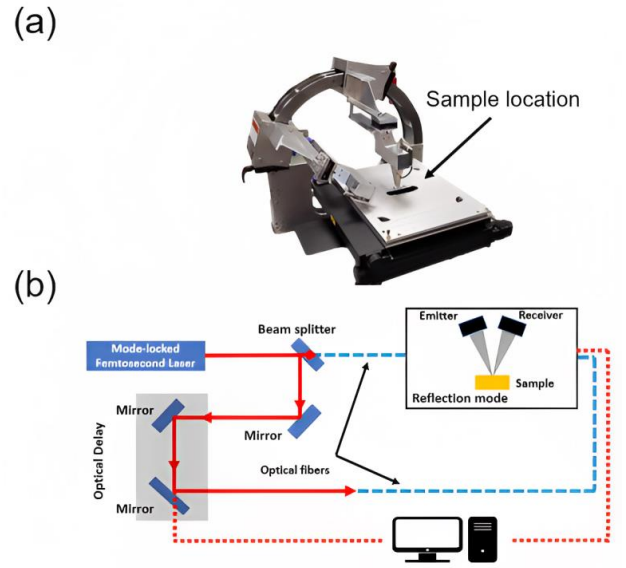

Fig. 2. (a). Photograph of stages for reflection experiments. (b). Schematic diagram of the experimental setup.

The THz measurements were carried out in an air-conditioned laboratory at 22^o C with humidity < 48%. Before the THz measurement, the reference pulse, *i.e.*, the THz pulse produced by the apparatus, was recorded by setting a bare metal plate (an excellent THz reflector) at the sample position. Balancing the transverse resolution and computational cost, these Roman amphora sherds were raster-scanned by a set of motorized stages moving in the *x*- and *y*- directions with step size 0.5 mm. The recorded reflected temporal signal at each pixel contains 4096 data points (corresponding sampling period T_s is 0.0116 ps) and is averaged over 10 shots per pixel to reduce the effect of noise. After completing the scanning, a 3D volume raw data set was acquired. The microstructure of the skin is examined with a ZEISS STEMI 2000-C stereo microscope.

IV. RESULTS AND DISCUSSION

Thickness measurements of skins were carried out first using optical microscopy with magnification 5×. Figure 3 presents one typical cross-sectional optical result of Roman amphora sherd from Northern Africa. Similar optical results are also found for Roman amphorae from Southern Spain and Southern Italy and are not presented here. The clay used for the production of the Northern Africa amphorae contains some ~50 μm large grains of impurities, which might be quartz, mica, or volcanic materials [3]. Moreover, as shown in Fig. 3, a whitish skin with a thickness of approximately 50 μm is found on the outer. Because the chemical deposition of calcite and NaCl is a quite complicated process, the skin thickness *L*

on the pinkish ceramic is not uniform.

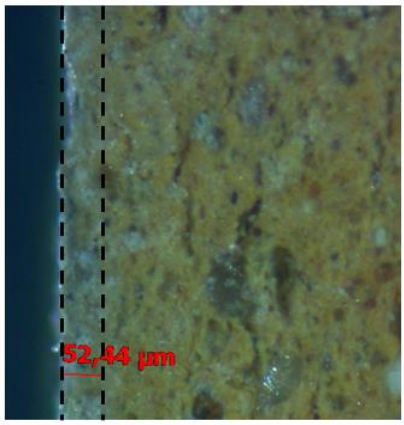

Fig. 3. Typical cross-sectional optical result of the Roman amphora sherd from Northern Africa. The two black dashed lines correspond to the air/skin and skin/body interface, respectively.

THz time-of-flight tomography (TOFT) was applied next for the nondestructive characterization of all Roman amphora sherds. High visual similarity of the waveform between the reflected signal and reference signal produced by the apparatus, is found. According to the effective bandwidth of the THz system utilized, the minimum optical thickness L in the air that can be resolved directly based on the raw temporal reflected signal is limited to ~100 μm, which is much larger than the skin thickness L observed in Fig. 3. Thus, an advanced signal processing approach is required to separate the overlapped echoes and reconstruct the stratigraphy of Roman amphora sherds hidden within the raw data.

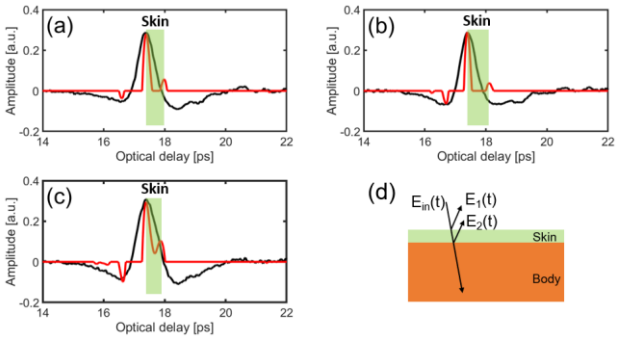

Fig. 4. Typical raw THz reflected signals (black) and the sparsity-based deconvolved signals (red) for Roman amphora sherds from (a) Northern Africa, (b) Southern Spain, and (c) Southern Italy. The green bar in (a)-(c) corresponds to the skin on Roman Amphora Sherds studied. Two positive echoes are resolved successfully by SD (red), while they are not visually evident in the raw reflected signal. (d) The origin of two echoes in the deconvolved signal; one from the air/skin interface, and the other from the skin/body interface.

According to our previous experience analyzing THz signals reflected from archaeological objects, the approach we resort to reconstructing the impulse response function associated with the investigated sample structure is sparse deconvolution based on the iterative shrinkage thresholding algorithm (SD/IST). Compared to conventional deconvolution approaches, such as frequency wavelet-domain deconvolution (FWDD) [14], in which the bandwidth of the impulse response function is narrowed because of the utilization of frequency-domain filtering to eliminate high- and low-frequency noises, sparse deconvolution is a pure time-domain technique that can provide a more clear representation of the impulse response function with limited sharp pulses. In addition, as a robust approach, the performance of the SD algorithm is less sensitive to the signal-to-noise ratio (SNR) of reference and reflected signals, making it quite suitable for practical applications. More details about the SD algorithm can be found in ref. [15,16].

Figure 4 shows the sparsity-based deconvolved signals of Roman amphora sherds from Northern Africa, Southern Spain, and Southern Italy. Compared with the raw reflected signal (black), two positive echoes, corresponding to the air/skin and skin/body interface, are clearly identified. The thickness L at that measured pixel can be calculated through the equation below,

$$L = c \times \Delta t / (2 \times n) \quad (1)$$

where c is the speed of light, n is the refractive index of skin in the THz band, and Δt is the optical delay between the two positive echoes in the SD-reconstructed signals. Assuming that the refractive index of skin is ~2 [13], the inferred skin thickness L is 44.37 μm for sherds from Northern Africa, 53.94 μm for sherds from Southern Spain, and 35.67 μm for sherds from Southern Italy, respectively. Overall agreement on L between optical and THz results is found.

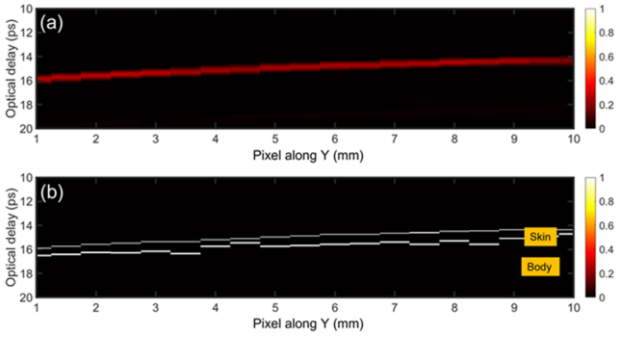

Fig. 5. Comparison of optical delay corresponding to skin on the body of Roman amphora sherd from Northern Africa between (a) the THz B-scan based on the raw data and (b) the binary THz B-scan based on the deconvolved data along the long axis of ROI in Fig. 1(a), in which a valid peak is assigned value "1" regardless the sign or height of the peak and other positions are assigned "0".

Finally, we reconstruct the detailed stratigraphy of the Roman amphora sherds through SD reconstructed signals. By performing a peak-detection (both positive and negative peaks), binary THz-B scans are obtained, in which a valid peak is assigned value "1" and the other position "0" regardless of the sign as well as the height of the peak. Figure 5(b) shows a binary B-scan of the rectangular region-of-interest (ROI) (Fig. 1) of the Roman amphora sherd from Northern Africa along the long axis. Similar results (not shown) were also found for Roman amphorae from Southern Spain and Southern Italy. Skin cannot be observed from the raw data in Fig. 5(a), while it is evident in Fig. 5(b), thus unlocking the detailed stratigraphic information after the application of SD. The optical distance between two nonzero positions in Fig. 5 varies, demonstrating that the physical thickness of skin on the Roman sherd from North Africa is nonuniform and position-dependent. The mean μ and standard deviation σ of skin thickness L are 30.06±7.55 μm for sherds from Northern Africa, 37.58±7.7 μm for sherds from Southern Spain, and 30.75±3.02 μm for sherds from Southern Italy, respectively.

V. CONCLUSION

In this work, THz time-of-flight tomography was used for the nondestructive evaluation of Roman amphora sherds from Northern Africa, Southern Spain, and Southern Italy. Sparse deconvolution based on an iterative shrinkage thresholding algorithm (SD/IST) was also implemented to beat the resolution of THz wavelength and enhance the resolution in depth. Echoes reflected from air/skin and skin/body interfaces are separated totally after SD, and the skin thickness L can be estimated based on the optical distance between the two positive echoes, which is L is 30.06±7.55 μm for sherds from Northern Africa, 37.58±7.7 μm for sherds from Southern Spain, and 30.75±3.02 μm for sherds from Southern Italy, respectively. The detailed stratigraphy of the Roman amphora sherds is also clearly revealed by sparsity-based THz reflectometry. Our analysis may provide valuable information to correlate sherds with kilns as well as to understand firing conditions and how they varied in space and time. Our work suggests a future large-scale study to establish such correlations.

REFERENCES

[1] C. Carreras, "Economía de la Britannia romana: la importación de alimentos", 1st edition, Instrumenta, 8, 2000.

[2] D.F. Williams, S.J. Keay, "Roman Amphorae: a digital resource." Archaeology data service, 2005.

[3] A.A. Nagy, G. Szakmány, "Amphorae as indicators of trade and diet in Cibalae (Pannonia)", ArcheoSciences. Revue, d'archométrie, no. 43-2, 2019, pp. 211-227.

[4] M.G. Fulford, D.P. Peacock, "The Avenue du President Habib Bourguiba, Salammbo: The Pottery and Other Ceramic Objects from the Site Excavations at Carthage: The British Mission I. 2", British Academy, University of Sheffield. vol. 96, 1984.

[5] J. Molera, T. Pradell, M. Vendrell-Saz, "The colors of Ca-rich ceramic pastes: Origin and characterization", Appl. Clay Sci. vol. 13, 1998, pp. 187-202.

[6] J. Dong, A. Locquet, M. Melis, D.S. Citrin, "Global mapping of stratigraphy of an old-master painting using sparsity-based terahertz reflectometry", Sci. Rep., vol. **7**, no. 1, 2017, pp. 1-12.

[7] K. Fukunaga, E. Cortes, A. Cosentino, I. Stuenkel, M. Leona, I.N. Duling, D.T. Mininberg, "Investigating the use of terahertz pulsed time domain reflection imaging for the study of fabric layers of an Egyptian mummy", J. Eur. Opt. Soc., vol. 6, 2011.

[8] J. Labaune, J.B. Jackson, S. Pagès-Camagna, I.N. Duling, M. Menu, G.A. Mourou, "Papyrus imaging with terahertz time domain spectroscopy", Appl. Phys. A. vol. 100, 2010, pp. 607-612.

[9] A. Bendada, S. Sfarra, C. Ibarra, M. Akhloufi, C. Pradere, X. Maldague, "Subsurface imaging for panel paintings inspection: a comparative study of the ultraviolet, the visible, the infrared and the terahertz spectra", Opto-electron. Rev., vol. 23, no. 1, 2015, pp. 90-101.

[10] S. Niijima, H. Taniguchi, K. Murate, K. Kawase, "Terahertz Spectroscopy Applied to Estimation of Firing Temperatures of Ancient Ceramics", IEEE Trans. Terahertz Sci. Technol., vol. 12, no. 3, 2022, pp. 300-306.

[11] K. Fukunaga, Y. Ogawa, S.I. Hayashi, I. Hosako, "Application of terahertz spectroscopy for character recognition in a medieval manuscript", IEICE Electron. Expr., vol. 5, no. 7, pp. 223-228, 2008.

[12] K. Fukunaga, I. Hosako, M. Palazzo, L. Dall'Aglio, F. Aramini, C. Cucci, M. Picollo, T. Ikari, I.N. Duling, "Terahertz time-domain imaging of "The Last Supper", In2020 45th International Conference on Infrared, Millimeter, and Terahertz Waves (IRMMW-THz), 2020, pp. 1-2.

[13] M. Mikerov, R. Shrestha, P. van Dommelen, D.M. Mittleman, M. Koch, "Analysis of ancient ceramics using terahertz imaging and photogrammetry," Opt. Express, vol. 28, no. 15, 2020, pp. 22255-22263.

[14] Y. Chen, S. Huang, E. Pickwell-MacPherson, "Frequency-wavelet domain deconvolution for terahertz reflection imaging and spectroscopy," Opt. Express, vol. 18, no. 2, 2010, pp. 1177-1190.

[15] J. Dong, X. Wu, A. Locquet, D.S. Citrin, "Terahertz superresolution stratigraphic characterization of multilayered structures using sparse deconvolution," IEEE Transactions on Terahertz Science and Technology, vol. 7, no. 3, 2017, pp. 260-267.

[16] M. Zhai, D.S. Citrin, A. Locquet, “Terahertz nondestructive stratigraphic analysis of complex layered structures: reconstruction techniques,” J. Infrared Millim. Terahertz Waves, vol. 42, no. 9, 2021, pp. 929-946.